# Characterisation of Lewis acid sites on the (100) surface of $\beta$-$AlF_3$: *ab initio* calculations of $NH_3$ adsorption

C.L. Bailey[1], A. Wander[1], S. Mukhopadhyay[2], B.G. Searle[1] and N.M. Harrison[1,2]

[1]*Computational Science and Engineering Department,*

*STFC Daresbury Laboratory, Daresbury,*

*Warrington, Cheshire, WA4 4AD, United Kingdom*

[2]*Department of Chemistry, Imperial College London,*

*Exhibition Road, London, SW7 2AZ, United Kingdom*

## Abstract

The current study employs hybrid-exchange density functional theory to show that the Lewis base, $NH_3$, binds to the $\beta$-$AlF_3$ (100) surface with a binding energy of up to -1.96 eV per molecule. This is characteristic of a strong Lewis acid. The binding of $NH_3$ to the surface is predominately due to electrostatic interactions. There is only a small charge transfer from the $NH_3$ molecule to the surface. The binding energy as a function of coverage is computed and used to develop a lattice Monte Carlo model which is used to predict the temperature programmed desorption (TPD) spectrum. Comparison with experimental TPD studies of $NH_3$ from $\beta$-$AlF_3$ strongly suggests that these structural models and binding mechanisms are good approximations to those that occur on real $AlF_3$ surfaces.

## I. INTRODUCTION

Strong Lewis acid catalysts are widely used in a variety of industrial processes. These include the large scale production of chlorofluorocarbons (CFCs) and hydrofluorcarbons (HFCs) for a wide range of applications including aerosol propellants, refrigerants and solvents. Traditionally, homogeneous Swartz catalysts, based on antimony pentafluoride ($SbF_5$), have been used for such reactions. Recently high surface area (HS) $AlF_3$ has been synthesised and found to catalyse reactions that are usually only catalysed by very strong Lewis acids such as $SbF_5$[1]. HS-$AlF_3$ is a heterogeneous catalyst and is therefore a promising alternative to $SbF_5$ for use as an industrial catalyst[2,3,4].

$AlF_3$ exists in several different crystalline forms. Thermodynamically, the most stable phase is $\alpha$-$AlF_3$, which has a close packed structure and shows very little catalytic activity. The metastable $\beta$ phase has a more open structure of the hexagonal tungsten bronze (HTB) type. The surface of $\beta$-$AlF_3$ is known to catalyse many fluorine and chlorine exchange reactions[5,6,7]. Experimental studies, including X-ray absorption near-edge structure at the F K-edge[8], temperature programmed desorption of $NH_3$[9] and the temperature programmed dismutation reaction of $CCl_2F_2$[10], suggest that amorphous HS-$AlF_3$ has a structure closely related to $\beta$-$AlF_3$. An understanding of the atomic scale structure and adsorption properties of the $\beta$-$AlF_3$ surface may therefore enable a better understanding of the catalytic nature of both $\beta$-$AlF_3$ and HS-$AlF_3$.

Models of the $\beta$-$AlF_3$ surface have been suggested based on its chemical activity and the assumption that the (100) plane provides the dominant surface[11]. Consequently, we have previously used density functional theory (DFT) calculations to investigate the phase stability of $\beta$-$AlF_3$ (100) in contact with gaseous $F_2$, as a function of the partial pressure and temperature of the gas[12,13]. We have shown that two different surface terminations are stable and have virtually identical surface energies (approximately 0.85 $Jm^{-1}$). These surfaces were termed the T1 and T6 terminations. $AlF_3$ is highly ionic and consequently both terminations are stoichiometric[13]. The terminations both contain Al ions that are under-coordinated and we have suggested previously that these under-coordinated Al ions are Lewis acid sites[12].

The binding energy of $NH_3$ is commonly used to quantify the strength of a Lewis acid[14,15,16]. DFT calculations on the zeolite, Mordenite,[14] show a range of Lewis acid sites;

from very weak sites with $NH_3$ binding energies as small as -0.2 eV to very strong sites with binding energies of up to -1.7 eV. The DFT calculated binding energy of $NH_3$ to strong Lewis acid sites on the $V_2O_5$ (010)[17] surface is around -1.3 eV. Lewis acidity can also be characterised by the vibrational spectrum of an adsorbed species such as pyridine, CO or $CD_3CN$. However, the vibrational spectra of adsorbed $NH_3$ is not a reliable method of quantifying Lewis acidity, in part, because the vibrational frequencies are very sensitive to the formation of hydrogen bonds between the $NH_3$ molecules and the surface to which it adsorbs.

In this paper we use hybrid-exchange density functional theory (DFT) to calculate the binding energy of $NH_3$ to under-coordinated Al ions at the $\beta$-$AlF_3$ (100) T1 and T6 terminations[12]. The variation in binding energy as a function of $NH_3$ coverage is also studied. These results are used to develop a lattice Monte Carlo model in order to predict the temperature programmed desorption (TPD) spectra. Comparison with experimental TPD studies of $NH_3$ from $\beta$-$AlF_3$ provides strong evidence to support these models of the surface. The (010) plane of $\beta$-$AlF_3$ also has two low energy terminations. One of these terminations is lower in energy than the (100) terminations and in a recent analysis of the equilibrium crystallite morphology was found to dominate[18]. However, the local structure of this termination is similar to that of the (100) T6 termination. The other low energy (010) termination is similar to the (100) T1 termination. This occurrence of similar local structures on the termination of the (100) and (010) surfaces strongly suggests that the local structure of HS-$AlF_3$ may also have similar sites to those found on the $\beta$ surfaces. Consequently, although in this study we investigate the adsorption of $NH_3$ on the under-coordinated Al ions at the $\beta$-$AlF_3$ (100) terminations, it is likely that the conclusions drawn here will also be applicable to similar sites on the $\beta$ (010) and the HS-$AlF_3$ surfaces.

## II. METHODOLOGY

All calculations were performed using the CRYSTAL code[19] and the B3LYP hybrid exchange functional[20]. This functional has been shown to provide a reliable description of geometric and electronic structure and energetics in a wide range of materials[21]. Polarised triple valence Gaussian basis sets were used throughout. The Al and F basis sets were defined in our previous paper[18]. A 5-11G* basis set was used for H and a 7-311G* basis set was used for N. These were obtained from previous studies[22,23,24]. In the case of N, a

polarisation function of $d$ symmetry, with an exponent of 0.8 Bohr$^{-2}$ was added to allow greater flexibility in the basis set. The N and H basis sets are tabulated in table I.

Structures of the $\beta$-$AlF_3$ (100) T1 and T6 terminations were obtained from our previous studies[12,13]. In the current study $NH_3$ molecules were adsorbed above under-coordinated Al ions on the T1 and T6 terminations. Structures were then fully optimised using a combination of damped molecular dynamics and Broyden-Fletcher-Goldfarb-Shanno (BFGS)[25] optimisers as implemented in CRYSTAL. The atomic positions were allowed to relax in all directions consistent with the symmetry of the system. The structures were considered to be converged when the residual forces along all allowed symmetry directions were below $1.0\times10^{-4}$ Hartrees Bohr$^{-1}$. The counterpoise scheme[26] was used to estimate the basis set superposition error (BSSE) between the adsorbed $NH_3$ molecules and the surface.

The relative charges on the atoms were calculated using a Mulliken partition of the total charge density. This is a somewhat arbitrary choice since there is no unique method of performing the partition of the charge density. However, the choice of a given scheme is still extremely useful in comparing the results of calculations performed using similar basis sets[27]. Mulliken analysis therefore provides a useful tool for comparing charge distributions at surfaces before and after adsorption events occur.

Temperature programmed desorption was simulated using a lattice Monte Carlo model. The rate of desorption, $r_{\mathrm{des}}$, calculated using the Redhead equation[28], for a first order desorption process is

$$r_{\mathrm{des}} = \nu_0 \exp\left(-\frac{|\Delta E|}{RT}\right) \tag{1}$$

where $\nu_o$ is the escape attempt frequency of the molecule, $\Delta E$ is its binding energy (in J mol$^{-1}$), $R$ is the molar gas constant and $T$ is the temperature of the system. Determination of an accurate rate of desorption is dominated by the accuracy of the calculation of the binding energy. The attempt frequency, $\nu_0$ is estimated from a calculation of the vibrational frequency of the Al-N bond.

## III. RESULTS

### A. The T1 surface

The relaxed T1 termination, shown in figure 1, contains two rows of ions in which alternate Al ions are under-coordinated. The outer-most row of under-coordinated Al ions are labelled T1A sites and those on the alternate row, T1B sites. There is one T1A and one T1B site per unit cell. The outer-most F ions on these two rows are coordinated to one Al ion and are referred to as dangling F ions. Side views of the terminations after adsorption of $NH_3$ at half and full monolayer coverage are shown in figure 2. The Al-N bond length is 2.0 Å. The $NH_3$ molecules form hydrogen bonds with adjacent dangling F ions, the H-F bond length is 2.0 Å. These bond lengths are independent of adsorption site and coverage. A plan view of the T1 termination with a full monolayer coverage of $NH_3$ is shown in figure 3. Each $NH_3$ molecule has two $NH_3$ neighbours, with an N-N separation of 5.4 Å, the next nearest neighbours (nnn) have an N-N separation of 7.3 Å.

The binding energies of $NH_3$, as a function of the occupancy of neighbouring sites, are displayed in table II. Overall, the binding energies are approximately 0.1 eV greater for adsorption on T1A sites than on T1B sites. The binding energy per molecule decreases as the level of coverage of neighbouring sites is increased. This variation in binding energies will be discussed in section IV.

### B. The T6 surface

The T6 termination, shown in figure 4, contains two symmetric rows of under-coordinated surface Al ions per unit cell, which are separated by an open channel. Each of these Al ions is bound to a dangling F ion, which is free to rotate to either open or close the surface channel. There are four under-coordinated Al sites per unit cell on the T6 termination, twice as many as on the T1 termination. There are two ways by which $NH_3$ can bind to these under-coordinated Al ions, as shown in figure 4. $NH_3$ can adsorb above the Al ions, this results in the surface F ions rotating downwards, by approximately 35°; this adsorption site is referred to as a T6A site. Alternatively, $NH_3$ molecules can adsorb from below the dangling F ions, this results in the surface F ions rotating upwards, by approximately 45°; this adsorption site is referred to as a T6B site. Consequently, there are many different

ways of adsorbing $NH_3$ molecules within a unit cell; there are four sites and each site can adsorb a molecule in two possible ways. Initial calculations showed that if an $NH_3$ molecule is adsorbed from above (to a T6A site) then at the adjacent sites there is a strong preference for adsorption at T6B sites and *vice versa*. For example, if at full monolayer coverage the occupied sites are all T6A, all T6B or alternating T6A and T6B, then the binding energies are -0.52, -0.20 and -1.40 eV respectively. In what follows we therefore assume that the adsorption sites on the T6 termination alternate between T6A and T6B sites.

Side views of the adsorption geometries at half and full monolayer coverage are shown in figure 5. The N-Al bond length is 2.0 Å, the same as that for adsorption to the T1 termination. One of the $NH_3$'s hydrogens bonds to a nearby F ion with a bond length of around 2.0 Å. These bond lengths are independent of adsorption site and coverage. Figure 6 is a plan view of full monolayer coverage on this termination. Each molecule has five neighbours within a radius of 7.0 Å, as shown in figure 6. For a molecule adsorbed on an T6A site the five neighbours consist of two molecules adsorbed on adjacent T6A sites labelled as (I) in figure 6, two molecules adsorbed on adjacent T6B sites, labelled as (II) in figure 6 and one molecule that is adsorbed on the T6B site across the channel, labelled as (III) in figure 6. Similarly, for a molecule adsorbed on a T6B site, it has two neighbours on adjacent T6B sites, two neighbours on adjacent T6B sites and a neighbour on a T6A site across the channel.

The binding energies as a function of the occupation of these five nearest neighbour sites have been calculated for the adsorption of $NH_3$ on both T6A and T6B sites. There are 32 ways to occupy 5 sites ($2^5$), after removing symmetrically equivalent possibilities this is reduced to 20. The resulting binding energies are displayed in table III. The binding energy of $NH_3$ at a T6A (T6B) site is most sensitive to the occupancy of the nearest T6A (T6B) site. These variations in binding energy are discussed further in section IV.

### C. Temperature Programmed Desorption Simulations

The binding energy of $NH_3$ to the $\beta$-$AlF_3$ (100) T1 and T6 terminations is strongly dependent on the local coverage. To enable a comparison of these results with TPD data we have used lattice Monte Carlo simulations to predict the rate of desorption as the temperature is increased at a rate of 7.5 K $min^{-1}$. In these simulations the initial lattice represents a

full monolayer coverage on either the T1 or T6 termination. The simulations are performed using a periodic unit cell consisting of 250,000 adsorption sites and the desorption simulation is run five times for each termination. The probability of desorption from each site is calculated using equation 1, the DFT computed binding energies tabulated in tables II and III and the attempt frequency, $\nu_0$, that is estimated from the vibrational frequency of the Al-N bond. The frequency is computed by construction of the force constant matrix via finite differencing of the analytical gradients followed by diagonalisation of the resultant dynamical matrix. Analysis using a partial force constant matrix computed by displacing the atoms of the Al-$NH_3$ motif indicates that the Al-N stretch frequency varies by around 50 $cm^{-1}$ ($1.5\times10^{12}$ $s^{-1}$) as the adsorption site and surface coverage are varied. Determination of an accurate rate of desorption is dominated by the calculation of the binding energy hence a single representative frequency of $1.7\times10^{13}$ $s^{-1}$ was used in our lattice Monte Carlo simulations, calculated from the full force constant matrix of the T1 surface at full monolayer coverage. Simulations of desorption from the T1 termination take into account the occupancy of nearest and next nearest neighbour sites. The DFT calculation required when a single next nearest neighbour site is occupied is prohibitively expensive so this is approximated by the average binding energy of the cases where there are none or two nearest neighbours present. This is expected to be accurate to within, at worst, 0.04 eV, based on the binding energies calculated as a function of nearest neighbour occupancy. All other binding energies are taken directly from table II. On the T6 termination the occupancy of the five next nearest neighbours, shown in figure 6, are considered.

Figure 7 contains the predicted desorption curve from the $\beta$-$AlF_3$ (100) T1 and T6 terminations. The predicted spectra contains three peaks. These can be assigned to the superposition of two spectra from each termination, each containing two peaks, as shown in figure 7. The peak that occurs at the lower temperature from each termination is due to desorption at high local coverage while the peak that occurs at the higher temperature is due to desorption when most, or all, neighbouring sites are unoccupied. These peaks occur at around 220°C and 350°C from the T1 termination and at around 130°C and 220°C from the T6 termination. The two central peaks overlap. The peaks associated with desorption from the T1 termination occur at 80% and 23% of the initial coverage, the peaks associated with desorption from the T6 termination occur at 79% and 26% of the initial coverage.

## IV. DISCUSSION

The calculated binding energies range from -1.15 eV, for adsorption at high coverage on the T6 termination, to -1.96 eV for adsorption on the T1 termination at low coverage. These values are typical of those obtained for materials displaying strong Lewis acidity; for instance, the DFT calculated binding energy for $NH_3$ at strong Lewis acid sites on Mordenite is -1.7 eV[14] and on the $V_2O_5$(010) surface sites it is around -1.3 eV[17]. Therefore the $\beta$-$AlF_3$ surface shows characteristics of a strong Lewis acid material.

### A. Properties of $NH_3$ adsorption on $\beta$-$AlF_3$

The Mulliken charges on the nitrogen and hydrogen atoms in an isolated $NH_3$ molecule are -0.91 |e| and +0.30 |e| respectively. The charges on the N, H, and the surface Al and F ions after full monolayer adsorption on the T1 and T6 terminations are shown in table IV. The charges on the N and H were corrected for BSSE by subtraction of the following two terms. (1) The charge that is transferred to the N and H basis functions in a calculation of the $AlF_3$ surface in the configuration it adopts after adsorption of $NH_3$, in the presence of the $NH_3$ basis functions. (2) The increase in the charge on the N and H atoms of an $NH_3$ molecule in the configuration it adopts after adsorption, when it is calculated in the presence of the $AlF_3$ basis functions compared to when it is calculated in the absence of the $AlF_3$ basis functions. Analogous corrections for BSSE were made for the charges on the surface Al and F ions. After adsorption to the T1 termination, around 0.2 |e| is transferred from the $NH_3$ to the surface. This charge is transferred to the neighbouring F ions. There is no significant change in the charge on the Al adsorption site. On the T6 termination the transfer of charge is similar. Approximately 0.2 |e| is transferred from the $NH_3$ molecule to the neighbouring dangling and bridging F ions. In the absence of BSSE corrections the charge transfer from the $NH_3$ molecule is approximately 1.0 |e| and 0.8 |e| for the T1 and T6 terminations respectively.

Although the assignment of charge is sensitive to the charge partition method and basis sets that are used, it appears that the charge transfer that is observed on these $AlF_3$ surfaces is less than that which has been calculated on other Lewis acid surfaces[17,29]. For instance, it is reported that after adsorption on Lewis acid vanadium sites on the $V_2O_5$ (010) surface,

between 0.3 and 0.4 |e| is transferred from the $NH_3$ molecule to the surface[17]. Previous computational studies on molecular systems have shown that there is no correlation between the degree of charge transfer and binding energies, but that observed trends can be quantitatively explained using simple electrostatic models[30].

There is a large electrostatic potential above the exposed under-coordinated Al ions on the $\beta$-$AlF_3$ terminations. A simple model is adopted to estimate the electrostatic contribution to the binding energy. A single $NH_3$ molecule is removed from the surface and the electrostatic potential is computed at the points in space previously occupied by the N and H ions. The electrostatic contribution to the binding energy is then computed by multiplying this potential by the charge on the N and H atoms of an isolated $NH_3$ molecule computed at the structure of the adsorbed molecule. The resultant energies are displayed in table V for adsorption sites on the T1 termination, and in table VI for adsorption sites on the T6 termination, at a range of surface coverages. The electrostatic contribution is very large, hence this suggests that the total binding energy of the molecule to the surface is dominated by electrostatic interactions. The electrostatic energies are greater than the calculated binding energies, in part, because the repulsive forces between the $NH_3$ molecule and the surface are not considered in this analysis. The contribution to the binding energy of the relaxation of the adsorption site and $NH_3$ molecule is also neglected. This contribution reduces the energy of the system by around 0.7 eV on the T1 termination and between 0.7 eV and 0.9 eV on the T6 termination.

The $NH_3$ binding energies are greater for adsorption on the T1 termination than on the T6 termination. Previous calculations of the binding energy of HF and HCl to these terminations also resulted in larger binding energies to the T1 termination[31]. We previously suggested that this is due to the different local geometries of the under-coordinated Al ions on each of the terminations. On the T1 termination the under-coordinated Al ions are bound to 5 bridging F ions, hence we can consider this Al ion to be effectively coordinated to 2.5 F ions (each F ion is shared between two Al ions). The under-coordinated Al ions on the T6 termination are bound to 4 bridging F ions and one monodentate F ion[18], hence the effective coordination of this Al ion is 3.0 ($0.5\times4+1$). The under-coordinated Al ions on the T1 termination are therefore in a less stable chemical environment than those on the T6 termination. This may explain why the under-coordinated Al ions on the T1 termination bind $NH_3$ more strongly.

It was shown in sections III A and III B that the binding energy of $NH_3$ at a given site is strongly dependent on the occupancy of neighbouring sites. In general, the binding energy decreases as the $NH_3$ coverage increases. It is proposed that repulsive interactions between neighbouring $NH_3$ molecules account for the observed variations in binding energy. These interactions can either be direct, e.g. dipolar repulsion, or indirect, that is, surface mediated. In order to analyse this, the direct interactions are estimated as follows. A periodic array of $NH_3$ molecules, constrained in the positions they adopt after adsorption to the surface, is considered. An electric field is applied perpendicular to the plane of the molecular net with the field strength chosen to produce charges on the N and H ions similar to those found after adsorption on the $AlF_3$ surface. The energy per molecule of the net is calculated and the calculations are then repeated with alternate $NH_3$ ions removed. The difference in the energy per molecule is used to estimate the direct nearest neighbour interactions, the resultant energies are displayed in table VII. The total $NH_3$ binding energy decreases by approximately 0.3 eV per molecule when nearest neighbours are present. It can therefore be concluded that variations in the binding energy of $NH_3$ as a function of coverage are due to both direct and indirect interactions of similar magnitude.

### B. Temperature Programmed Desorption Simulations

Experimental TPD spectra for $NH_3$ on $\beta$-$AlF_3$ obtained by Kemnitz *et al*[9] are shown in figure 8. There are three distinct peaks/shoulders, at around 200°C, 300°C and 420°C. It is tempting to suggest that these three features correspond to the three peaks predicted from our lattice Monte Carlo simulations, shown in figure 7, even though the peaks/shoulders obtained from the experimental procedure occur at temperatures that are systematically around 70°C higher than those computed.

There are several factors which may cause this slight discrepancy in absolute temperatures. Experimentally it is difficult to increase the temperature uniformly at the surface and to measure it accurately. Consequently, the temperature of the surface may be over-estimated. In the Monte Carlo simulations it is assumed that there is no barrier to the desorption process, if this is not true, the temperature at which desorption occurs will be under-estimated in our simulations. In the DFT approach used here the calculations of relative binding energies are much more accurate than the absolute energies, yet, an error

in the absolute binding energy of 0.1 eV changes the temperature at which peak desorption occurs by approximately 30°C. It is known that hydrolysis and hydroxylation occurs at the surface of real samples of $\beta$-$AlF_3$[5], two of the experimental samples have been fluorinated to limit hydroxylation and hydration of the surface, however, it can clearly be seen that the TPD of $NH_3$ is sensitive to such factors. Despite the effects of these possible errors and approximations, it is very encouraging to see that the predicted relative temperatures at which desorption peaks occur are in extremely good agreement with those observed.

The simulation of TPD from the (100) surface suggests that the predicted local surface geometries are representative of the geometries that occur on real $\beta$-$AlF_3$ surfaces. Furthermore, the ability to assign TPD peaks to the local structure of adsorption sites may provide a method for studying how different synthesis methods affect the local structure of $\beta$-$AlF_3$ and HS-$AlF_3$ surfaces. For example, from figure 8 it can be seen that the experimental sample that was post fluorinated with $CHClF_2$ has a more defined shoulder at low temperatures compared to the other samples. The analysis developed here implies that this is because the sample's surface presents more sites of the type seen on the T6 termination. This study also illustrates that even the number of different adsorption sites at an $AlF_3$ surface cannot be derived directly from the TPD spectra as the analysis requires a careful consideration of the coverage dependence of the adsorption energies.

## V. CONCLUSIONS

We have shown that $NH_3$ binds strongly to under-coordinated Al ions on the $\beta$-$AlF_3$ (100) surface. Our calculated binding energies are typical of values obtained for strongly Lewis acidic zeolite materials. We have shown that the binding energy is predominately due to the interaction of the $NH_3$ with the large electrostatic potential above the under-coordinated Al ions. The binding energy of $NH_3$ was shown to decrease with increased surface coverage, due to a combination of direct repulsive interactions between neighbouring $NH_3$ molecules and a surface mediated interaction due to surface relaxations upon adsorption. We have simulated the TPD spectrum for the $\beta$-$AlF_3$ (100) T1 and T6 terminations and compared our results with experimental TPD data. Our results suggested that the types of local sites seen on the T1 and T6 terminations occur on real $\beta$-$AlF_3$ surfaces and that the structural models and binding mechanisms described here are a close approximation to those which

occur on real $AlF_3$ surfaces.

## VI. ACKNOWLEDGEMENTS

We would like to thank Professor Erhard Kemnitz for invaluable discussions and for the experimental data obtained by his group at the Humboldt University in Berlin that is discussed in this paper. We thank the EU for support of part of this work through the $6^{th}$ Framework Programme (FUNFLUOS, Contract No. NMP3-CT-2004-5005575). The calculations were performed in part on STFC's SCARF and NW-Grid systems and in part on the HPCx system where computer time has been provided via our membership of the UK's HPC Materials Chemistry Consortium and funded by EPSRC (portfolio grant EP/D504872).

---

[1] E. Kemnitz, U. Groß S. Rüdiger, and S. C. Shekar. *Angew. Chem.*, 115:4383, 2003.

[2] G.B. McVicker, C.J. Kim, and J.J. Eggert. *J. Catal.*, 80:315, 1983.

[3] E. DeCanio, J.W. Bruno, V.P. Nero, and J.C. Edwards. *J. Catal.*, 140:84, 1993.

[4] E. Kemnitz and D.H. Menz. *Prog. Solid State Chem.*, 26:97, 1998.

[5] A. Hess and E. Kemnitz. *J. Catal.*, 149:449, 1994.

[6] A. Hess, E. Kemnitz, A. Lippitz, W.E.S. Unger, and D.H. Menz. *J. Catal.*, 148:270, 1994.

[7] N. Herron and W.E. Farneth. *Adv. Mater.*, 8:959, 1996.

[8] S.L.M. Schroeder and N. Weiher. *Phys. Chem. Chem. Phys.*, 8:1807, 2006.

[9] J.K. Murthy, U. Groß S. Rüdiger, V.V. Rao, V.V. Kumar, A. Wander, C.L. Bailey, N.M. Harrison, and E. Kemnitz. *J. Phys. Chem. B*, 110:8314, 2006.

[10] E.K.L.Y. Hajime, J.L. Delattre, and A.M. Stacy. *Chem. Mater.*, 19:894, 2007.

[11] E. Kemnitz, A. Kohne, I. Grohman, A. Lippitz, and A.W.S. Unger. *J. Catal.*, 159:270, 1996.

[12] A. Wander, C.L. Bailey, B.G. Searle, S. Mukhopadhyay, and N.M. Harrison. *Phys. Chem. Chem. Phys.*, 7:3989, 2005.

[13] A. Wander, C.L. Bailey, S. Mukhopadhyay, B.G. Searle, and N.M. Harrison. *J. Mater. Chem.*, 16:1906, 2006.

[14] L. Benco, T. Bučko, J. Hafner, and H. Toulhoat. *J. Phys. Chem. B*, 108:13656, 2004.

[15] M. Elanany, M. Koyama, M. Kubo, E. Broclawik, and A. Miyamoto. *Applied Surf. Sci.*, 246:96, 2005.

[16] A.A. Lamberov, A.M. Kuznetsov, M.S. Shapnik, A.N. Masliy, S.V. Borisevich, R.G. Romanova, and S.R. Egorova. *J. Mol. Catal. A*, 158:481, 2000.

[17] X. Yin, H. Han, A. Endou I. Gunj and, S.S.C. Ammal, M. Kubo, and A. Miyamoto. *J. Phys. Chem. B*, 103:4701, 1999.

[18] A. Wander, C.L. Bailey, S. Mukhopadhyay, B.G. Searle, and N.M. Harrison. *in press J. Phys. Chem. C*, 2008.

[19] R. Dovesi, V.R. Saunders, C. Roetti, R. Orlando, C.M. Zicovich-Wilson, F. Pascale, B. Civalleri, K. Doll, N.M. Harrison, I.J. Bush, P. D'Arco, and M. Llunell. *CRYSTAL 2006 Users's Manual*. University of Torino, 2007.

[20] A.D. Becke. *J. Chem. Phys.*, 98:1372, 1993.

[21] J. Muscat, A. Wander, and N.M. Harrison. *Chem. Phys. Letts.*, 342:397, 2001.

[22] Basis sets are available from http://www.tcm.phy.cam.ac.uk/ mdt26/crystal.html.

[23] R. Dovesi, C. Ermondi, E. Ferrero, C. Pisani, and C. Roetti. *Phys. Rev. B*, 29:3591, 1984.

[24] R. Pandey, J.E. Jaffe, and N.M. Harrison. *J. Chem. Phys. Solids*, 55:1357, 1994.

[25] P. Spellucci. Available from http://plato.asu.edu/sub/nlounres.html. University of Darmstadt.

[26] S.F. Boys and F. Bernardi. *Mol. Phys.*, 19:553, 1970.

[27] C. Pisani, R. Dovesi, and C. Roetti. Hartree-fock ab initio treatment of crystalline systems. *Lecture Notes in Chemistry*, 48, 1988.

[28] P.A. Readhead. *Vacuum*, 12:203, 1962.

[29] T. Bučko, J. Hafner, and L. Benco. *J. Chem. Phys.*, 120:10263, 2004.

[30] A.Y. Timoshkin, A.V. Suvorov, H.F. Bettinger, and H.F. Schaefer. *J. Am. Chem. Soc.*, 121:5687, 1999.

[31] C.L. Bailey, S. Mukhopadhyay, A. Wander, and N.M. Harrison. *in press Phys. Chem. Chem. Phys.*, DOI: 10.1039/b718733e, 2008.

**Fig. 1** A side view (left) and a plan view (right) of the relaxed $\beta$-$AlF_3$ (100) T1 termination. The Al ions are represented by small spheres and the F ions by large spheres.

**Fig. 2** Adsorption of $NH_3$ above under-coordinated Al ions on the $\beta$-$AlF_3$ (100) T1 termination. (a) Adsorption on T1A sites. (b) Adsorption on T1B sites. (c) Adsorption on T1A and T1B sites.

**Fig. 3** A plan view of $NH_3$ adsorption on the $\beta$-$AlF_3$ (100) T1 termination at full monolayer coverage. There are two adsorbed $NH_3$ molecules per unit cell. The channels in the bulk material are parallel to the <001> direction.

**Fig. 4** The $\beta$-$AlF_3$ (100) T6 termination. $NH_3$ can either bind to the surface Al ions from above (on T6A sites) or below (on T6B sites).

**Fig. 5** Adsorption of $NH_3$ above under-coordinated Al ions on the $\beta$-$AlF_3$ (100) T6 termination. (a) Adsorption on T6A sites. (b) Adsorption on T6B sites. (c) Adsorption on T6A and T6B sites.

**Fig. 6** A plan view of $NH_3$ adsorption on the $\beta$-$AlF_3$ (100) T6 termination at full monolayer coverage. There are four $NH_3$ molecules adsorbed per unit cell. Arrows point to the five nearest neighbours of an T6A and T6B site. The neighbouring adsorption sites for a molecule adsorbed to a T1A (T6B) site are labelled as: (I) nearby T6A (T6B) site, (II) adjacent T6B (T6A) site and (III) T6B (T6A) site across the channel. The channels in the bulk material are parallel to the <001> direction.

**Fig. 7** The TPD curves obtained from lattice Monte Carlo simulations parameterised from the $NH_3$ DFT binding energies.

**Fig. 8** The TPD curves obtained by Kemnitz *et al.* (Left) The three experimental results were obtained from different $\beta$-$AlF_3$ samples. Experiment A used untreated $\beta$-$AlF_3$, experiment B used a $\beta$-$AlF_3$ sample that was first fluorinated using $CCl_2F_2$ and in experiment C the sample was fluorinated using $CHClF_2$. The fluorination process is used to reverse surface hydrolysis. (Right) This graph is identical to

the one on the left but also includes the results obtained from our lattice Monte Carlo simulations, shifted by 70°C to higher temperatures.

*TABLE I: The basis sets used for nitrogen and hydrogen.*

| | Nitrogen | | |
|---|---|---|---|
| Orbital | Exp. | s co-eff | p co-eff |
| 1s | 7590 | 0.000889 | |
| | 991.2 | 0.008994 | |
| | 190.1 | 0.05287 | |
| | 52.69 | 0.1710 | |
| | 18.10 | 0.3612 | |
| | 7.048 | 0.4027 | |
| 2sp | 18.40 | -0.02807 | 0.01869 |
| | 4.242 | -0.1146 | 0.10130 |
| | 1.347 | 0.1890 | 0.2394 |
| 3sp | 0.422 | 1.0 | 1.0 |
| 4sp | 0.113 | 1.0 | 1.0 |
| 3d | 0.8 | 1.0 (d co-eff.) | |

| | Hydrogen | |
|---|---|---|
| Orbital | Exp. | s co-eff |
| 1s | 50362.3 | 0.00000020 |
| | 29510.2 | 0.00000104 |
| | 4251.44 | 0.00001154 |
| | 827.084 | 0.00007679 |
| | 193.406 | 0.00043129 |
| | 50.0397 | 0.00219849 |
| | 13.7402 | 0.01055974 |
| | 3.9009 | 0.04760939 |
| 2s | 1.1397 | 0.18487289 |
| | 0.346 | 0.47812170 |
| 3s | 0.109 | 1.0 |
| 2p | 0.1098 | 1.0 (p co-eff) |

*TABLE II: Binding energies (BE), in eV per molecule, of $NH_3$ as a function of the occupation of neighbouring and next nearest neighbouring (nnn) sites. Nearest neighbour sites are of an opposite site type while next nearest neighbour sites are of the same type.*

| Adsorption site | No. of nearest neighbours | BE with no nnn (eV) | BE with both nnn (eV) |
|---|---|---|---|
| T1A | 0 | -1.96 | -1.86 |
| T1A | 1 | -1.86 | -1.68 |
| T1A | 2 | -1.72 | -1.54 |
| T1B | 0 | -1.86 | -1.77 |
| T1B | 1 | -1.75 | -1.64 |
| T1B | 2 | -1.57 | -1.50 |

*TABLE III: Binding energies (BE) of $NH_3$ adsorbed to the T6 termination as a function of the occupancy of the its nearest neighbour sites. The nearest neighbour sites are described in detail in the section III B and shown diagrammatically in figure 6*

| Adsorption on T6A sites | | | | Adsorption on T6B sites | | | |
|---|---|---|---|---|---|---|---|
| Binding Energy (eV) | No. of $NH_3$ at nearby T6A sites | No. of $NH_3$ at adjacent T6B sites | No. of $NH_3$ at T6B sites across the channel | Binding Energy (eV) | No. of $NH_3$ at nearby T6B sites | No. of $NH_3$ at adjacent T6A sites | No. of $NH_3$ at T6A sites across the channel |
| -1.55 | 0 | 2 | 1 | -1.62 | 0 | 1 | 1 |
| -1.54 | 0 | 0 | 0 | -1.60 | 0 | 0 | 0 |
| -1.51 | 0 | 2 | 0 | -1.57 | 0 | 2 | 0 |
| -1.46 | 0 | 1 | 0 | -1.55 | 0 | 1 | 0 |
| -1.45 | 0 | 1 | 1 | -1.51 | 0 | 2 | 1 |
| -1.45 | 0 | 0 | 1 | -1.51 | 0 | 0 | 1 |
| -1.40 | 1 | 2 | 1 | -1.45 | 1 | 1* | 1 |
| -1.34 | 1 | 1* | 0 | -1.44 | 1 | 1** | 1 |
| -1.34 | 1 | 1** | 1 | -1.40 | 1 | 0 | 0 |
| -1.33 | 1 | 0 | 0 | -1.39 | 1 | 0 | 1 |
| -1.31 | 1 | 0 | 1 | -1.38 | 1 | 2 | 0 |
| -1.29 | 1 | 1* | 1 | -1.32 | 2 | 2 | 1 |
| -1.27 | 1 | 2 | 0 | -1.31 | 1 | 2 | 1 |
| -1.26 | 1 | 1** | 0 | -1.31 | 2 | 1 | 1 |
| -1.24 | 2 | 2 | 1 | -1.30 | 2 | 2 | 0 |
| -1.23 | 2 | 0 | 0 | -1.29 | 1 | 1* | 1 |
| -1.22 | 2 | 2 | 0 | -1.24 | 1 | 1** | 0 |
| -1.18 | 2 | 1 | 1 | -1.25 | 2 | 0 | 1 |
| -1.17 | 2 | 0 | 1 | -1.21 | 2 | 0 | 0 |
| -1.15 | 2 | 1 | 0 | -1.18 | 2 | 1 | 0 |

* The T6A site and T6B site that are occupied are adjacent to one another

**The T6A site and T6B site that are occupied are not adjacent to one another

*TABLE IV: The Mulliken charges on the different surface species at full monolayer coverage, after correction for BSSE. The changes in the charges are given with respect to the clean surface and an isolated $NH_3$ molecule. An isolated $NH_3$ molecule has a charge of -0.91 on the nitrogen and +0.30 on the hydrogens.*

| Species | T1 A | T1 B | T6 A | T6 B |
|---|---|---|---|---|
| N | -0.91 | -0.91 | -0.88 | -0.90 |
| H | 0.37 | 0.37 | 0.35 | 0.39 |
| H | 0.36 | 0.36 | 0.35 | 0.36 |
| H (H bonded) | 0.38 | 0.38 | 0.38 | 0.34 |
| $\Delta$ $NH_3$ | 0.20 | 0.19 | 0.18 | 0.19 |
| $\Delta$ Al | -0.02 | -0.02 | 0.01 | 0.01 |
| $\Delta$ bridging Fs* | -0.13 | -0.10 | -0.08 | -0.08 |
| $\Delta$ dangling F | -0.05 | -0.08 | -0.12 | -0.13 |

* The Al adsorption sites on the T1 termination are bound to 5 bridging Fs and on the T6 termination they are bound to 4 bridging Fs.

*TABLE V: Estimations of the electrostatic interaction energy between the T1 termination and adsorbed $NH_3$ molecules. The calculated binding energies are given for comparison.*

| Binding site | Binding energy (eV) | Electrostatic interaction (eV) | Occupied neighbouring sites |
|---|---|---|---|
| T1A | -1.96 | -2.20 | None |
| T1A | -1.86 | -2.13 | One at nearby B site |
| T1A | -1.72 | -2.04 | Two at nearby B sites |
| T1B | -1.86 | -2.14 | None |
| T1B | -1.75 | -2.04 | One at nearby A site |
| T1B | -1.57 | -1.96 | Two at nearby A sites |

*TABLE VI: Estimations of the electrostatic interaction energy between the T6 termination and adsorbed $NH_3$ molecules. The calculated binding energies are given for comparison.*

| Binding site | Binding energy (eV) | Electrostatic interaction (eV) | Occupied neighbouring sites |
|---|---|---|---|
| T6A | -1.54 | -1.98 | None |
| T6A | -1.33 | -1.82 | One at a nearby A site |
| T6A | -1.23 | -1.80 | Two at nearby A sites |
| T6B | -1.60 | -2.21 | None |
| T6B | -1.40 | -2.07 | One at a nearby B site |
| T6B | -1.21 | -2.03 | Two at nearby B sites |

*TABLE VII: Estimation of the repulsive dipole interaction energy between neighbouring $NH_3$ molecules in the absence of the $AlF_3$ surface. The termination and adsorption sites describe the positioning of the $NH_3$ molecules. The interaction energy includes the interactions from both nearest neighbours.*

| Termination | Adsorption sites | Dipole Interaction (eV) |
|---|---|---|
| T1 | T1A+T1B | 0.056 |
| T6 | T6A | 0.044 |
| T6 | T6B | 0.052 |

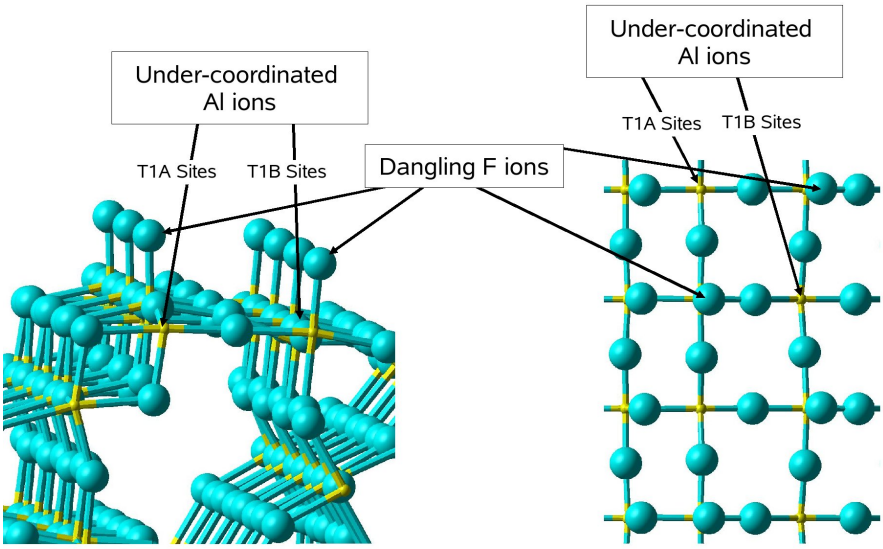
Under-coordinated
Al ions
T1A Sites
T1B Sites
Dangling F ions
Under-coordinated
Al ions
T1A Sites
T1B Sites

*FIG. 1:*

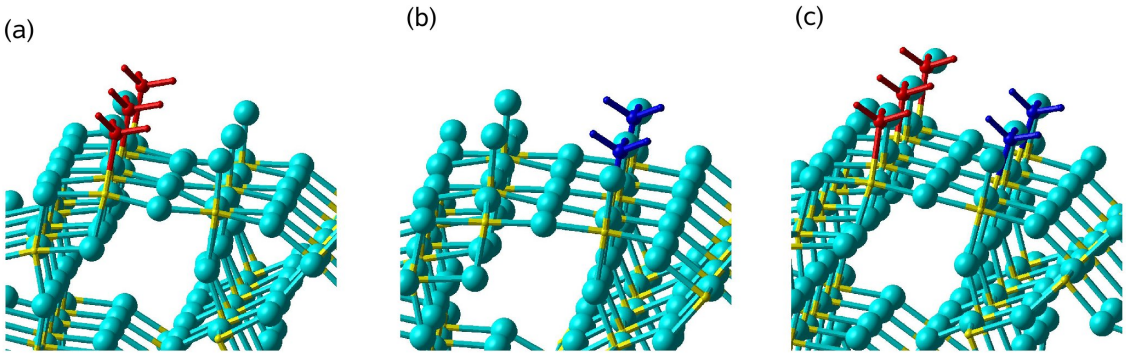
(a)
(b)
(c)

*FIG. 2:*

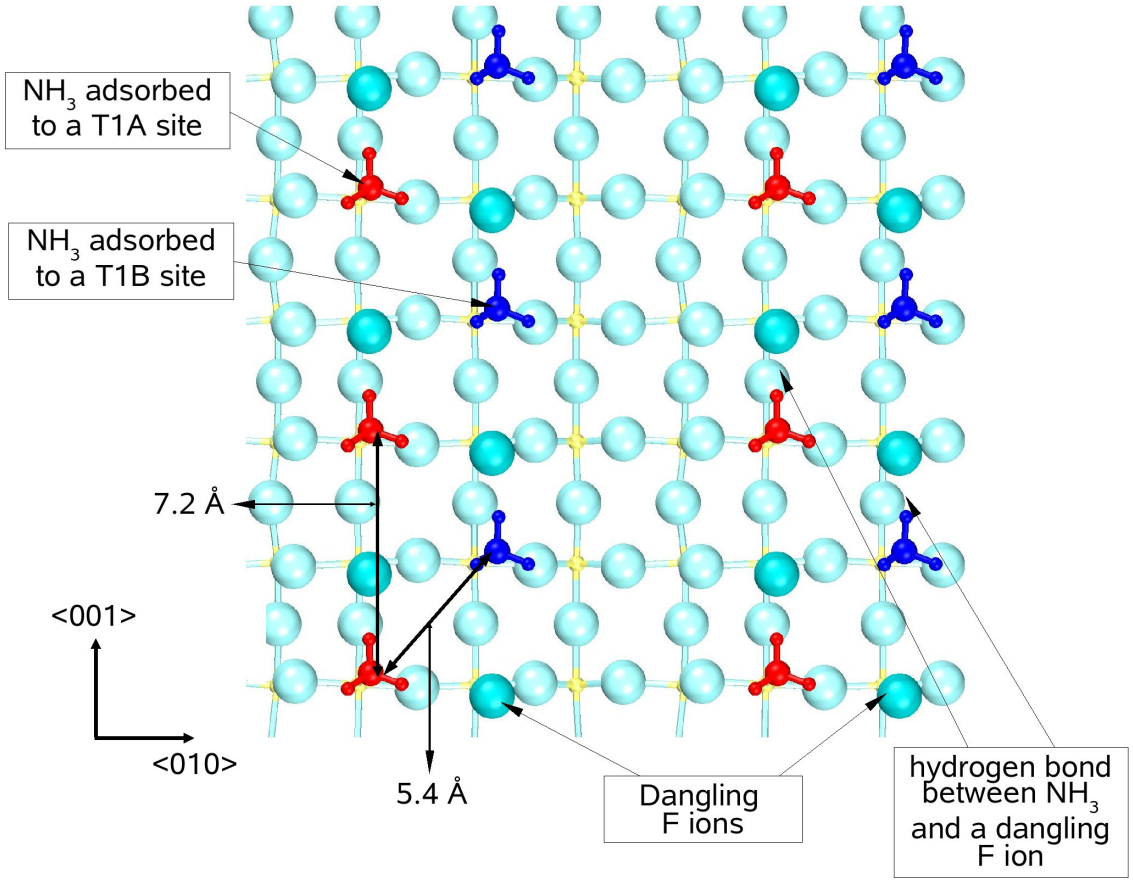
NH3 adsorbed to a T1A site
NH3 adsorbed to a T1B site
7.2 Å
<001>
<010>
5.4 Å
Dangling F ions
hydrogen bond between NH3 and a dangling F ion

*FIG. 3:*

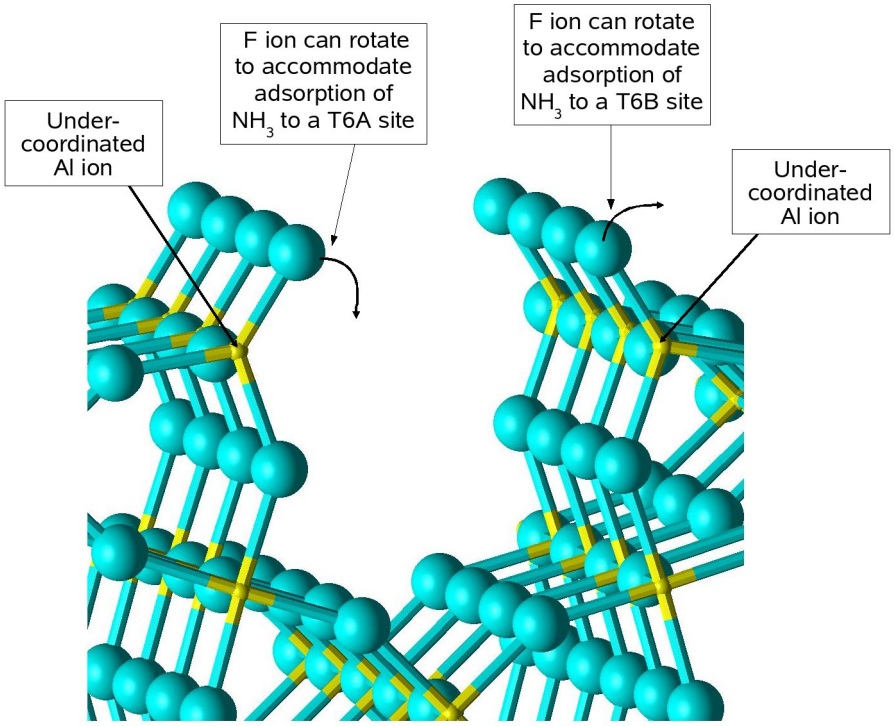
F ion can rotate to accommodate adsorption of $NH_3$ to a T6A site
F ion can rotate to accommodate adsorption of $NH_3$ to a T6B site
Under-coordinated Al ion
Under-coordinated Al ion

*FIG. 4:*

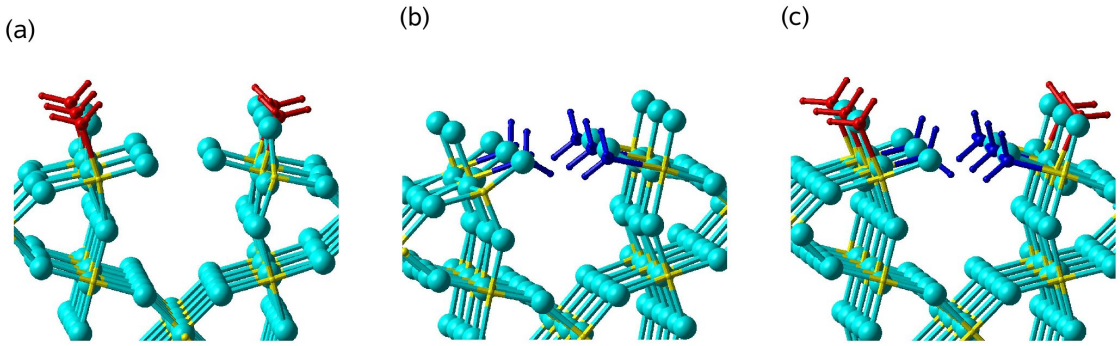
(a)
(b)
(c)

*FIG. 5:*

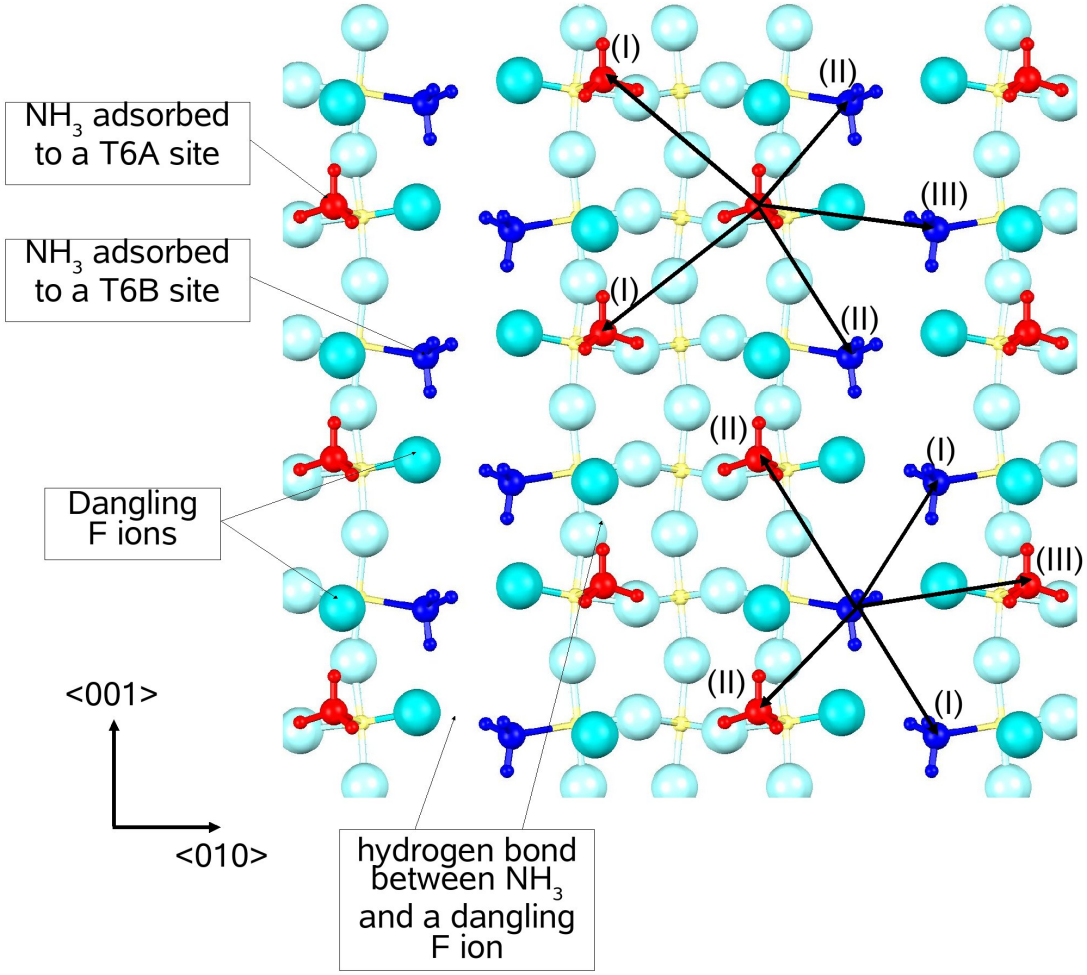
NH3 adsorbed to a T6A site
NH3 adsorbed to a T6B site
Dangling F ions
<001>
<010>
hydrogen bond between NH3 and a dangling F ion
(I)
(II)
(III)
(I)
(II)
(II)
(I)
(III)
(II)
(I)

*FIG. 6:*

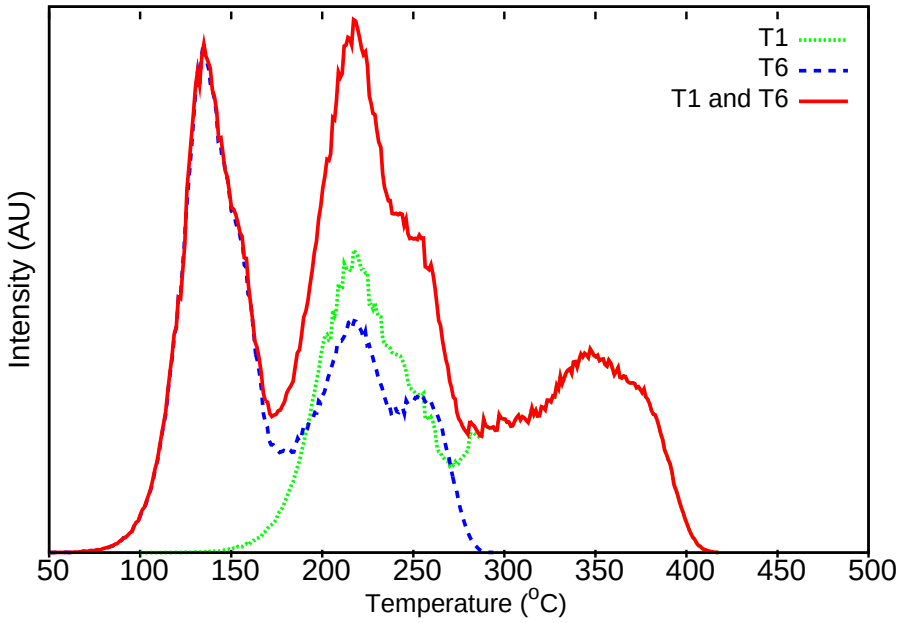
T1
T6
T1 and T6
Intensity (AU)
50
100
150
200
250
300
350
400
450
500
Temperature (°C)

*FIG. 7:*

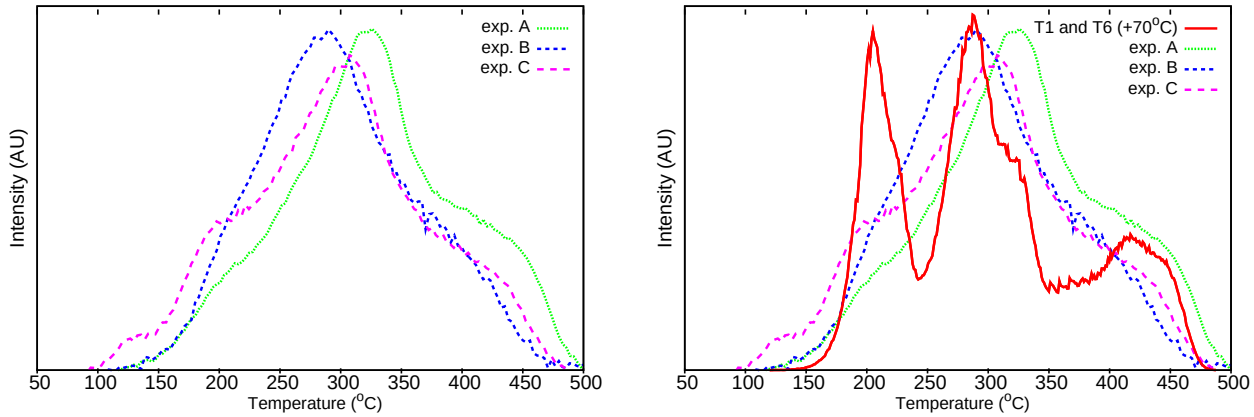
exp. A
exp. B
exp. C
Intensity (AU)
50
100
150
200
250
300
350
400
450
500
Temperature (°C)
T1 and T6 (+70°C)
exp. A
exp. B
exp. C
Intensity (AU)
50
100
150
200
250
300
350
400
450
500
Temperature (°C)

*FIG. 8:*